PLA NANOPARTICLES LOADED WITH THYMOL TO IMPROVE ITS INCORPORATION INTO GELATINE FILMS

Sara Sáez-Orviz, Ismael Marcet, Shihan Weng, Manuel Rendueles*, Mario Díaz.

a Department of Chemical and Environmental Engineering, University of Oviedo. C/ Julián Clavería 8, 33006 Oviedo (Spain).

*Corresponding author. Tel: +34-985106226. Fax: +34-985103434. Email: mrenduel@uniovi.es

ABSTRACT

Thymol is an active agent with remarkable antimicrobial properties but with low solubility in water and is able to exert a negative effect on the mechanical properties of protein-based films. Furthermore, it is highly volatile and during the drying of the film-forming solution it may be lost through evaporation, a question that has barely been studied.

In a previous investigation, the encapsulation of thymol using PLA was optimized, and, in the present study, these PLA nanoparticles are incorporated into gelatine films to assess their effect on the film properties and thymol evaporation during the drying of the film-forming solution.

At the thymol concentrations tested, all the free thymol was completely evaporated during the drying of the film-forming solution, while a part of the thymol encapsulated in PLA nanoparticles remained in the gelatine film matrix. The gelatine films with PLA-thymol nanoparticles showed high transparency, a homogeneous microstructure and antimicrobial properties.

1. INTRODUCTION

Films made using natural biopolymers can be used directly on food and they have several functions, such as forming a physical separation between food and the environment (avoiding food spoilage due to pollution or the presence of microorganisms in the media), decreasing food dryness due to water evaporation, maintaining the organoleptic characteristics of the food and, in short, increasing food shelf-life. In order to fulfil these objectives, films have to possess certain characteristics: they have to be water-resistant, improve food appearance, be easily manipulated, have low viscosity, resist mechanical pressure to some extent, and be able to carry active agents (Dhall, 2013). These types of films are usually made up of a plasticiser and a biopolymer solubilised in a common solvent. This solution is cast in a mould and the

solvent is evaporated with, or sometimes without, the application of heat. Among the biopolymers seen as candidates for preparing these films are some polysaccharides, such as starch (Bonilla et al., 2013; Dang and Yoksan, 2016; Nouri and Nafchi, 2014), and proteins, such as the gelatine (Arfat et al., 2014; Etxabide et al., 2017; Tongnuanchan et al., 2014). Gelatine is produced by the hydrolysis of animal collagen, so it can be obtained inexpensively from a wide variety of sources. Furthermore, gelatine shows excellent biocompatibility, biodegradability and non-toxicity and it can be used to prepare edible films capable of carrying different active agents (Etxabide et al., 2017).

Among the active agents that have received the attention of the research community, thymol can be highlighted due to its major antimicrobial properties. Thymol is obtained from essential oils of plants of the family Lamiaceae, such as the genus *Thymus, Ocimum, Origanum, Satureja, Thymbra* and *Monarda*. When pure, it is a crystalline substance with a characteristic scent. Thymol and other compounds that are present in essential oils have been registered by the Food and Drug Administration (FDA) as *Generally Recognised as Safe* (GRAS), and due to their harmlessness and to their medicinal properties, they have also attracted the interest of the food industry. However, thymol has some disadvantages that hinder its direct use in foods, since it is a highly volatile compound, with low solubility in water and high solubility in ethanol and other organic solvents and highly degraded by the light. Principally as a result of these inconveniences, the incorporation of this active agent into edible films could be considered problematic. If thymol is added to the film-forming solution, its low solubility in water could lead to its aggregation during the solvent evaporation stage, producing a deterioration of the film matrix, and therefore, a decrease in the mechanical properties of the films obtained. This problem can be solved by solubilising the thymol in a solvent of high-ethanolic content, such as that required to solubilise the protein zein. Films made with this protein and thymol have been widely reported by several authors (Del Nobile et al., 2008; Li et al., 2012; Mastromatteo et al., 2009; Park et al., 2012). Furthermore, during the solvent evaporation stage, the high volatility of thymol could lead to its partial or total evaporation, a question that has scarcely been investigated and which is of great interest when considering the possibility of introducing thymol as an additive in protein-based films in order to take advantage of its desirable properties. Kavoosi et al. (2013) produced gelatine films with thymol and in their study the mechanical properties of the film were reinforced using glutaraldehyde, a toxic crosslinker that cannot be allowed to come into contact with food. Despite the use of this crosslinker, the addition of thymol produced a noticeable decrease in the mechanical properties of the film.

In recent research, Marcet et al. (2018) described the preparation and characterisation of polylactic acid (PLA) nanoparticles loaded with thymol. PLA is a biodegradable and biocompatible polymer that has been used by several authors to encapsulate other natural antioxidants from plants, such as vanillin (Dalmolin et al., 2016) or aureusidin (Roussaki et al., 2014). The addition of these nanoparticles loaded with thymol to the film-forming solution of a protein-based film could solve two problems: first of all, it could potentially hinder the loss of thymol during the evaporation step and furthermore, it might avoid the structural changes in the film matrix caused by the active agent when it is free in the solution.

So, in this investigation, the PLA nanoparticles loaded with thymol that were reported in previous work (Marcet et al., 2018) were incorporated into gelatine films. The amount of thymol that remained in the film matrix after the film-forming solution drying step, the mechanical properties, microstructure, thymol release behaviour and antioxidant properties of these gelatine films were evaluated. Furthermore, the antimicrobial properties of the films obtained were tested using apple pieces previously inoculated with *Escherichia coli*.

2. MATERIALS AND METHODS

2.1. Materials

The following reagents were acquired from Sigma-Aldrich (St Louis, USA): thymol (ref. T0501), gelatine from porcine skin (ref. G1890), glycerol (ref. G7893), magnesium nitrate (ref. 237175). The Nutrient Broth (NB, ref. 70149NB) and ethanol 96% (ref.83804.360) were acquired from VWR (Pennsylvania, USA).

2.2. Preparation of PLA nanoparticles loaded with thymol

The PLA nanoparticles loaded with thymol were prepared using the single emulsion preparation technique, a procedure reported in previous work (Marcet et al., 2018). This previous study showed that the nanoparticles able to encapsulate the highest amount of active agent were those prepared by dissolving 150 mg of thymol and 150 mg of PLA in 7.5 mL of dichloromethane. This solution was then emulsified by ultrasound in 30 mL of a polyvinyl alcohol solution. The nanoparticles thus prepared were spherical in shape and had an average size of 244.6 ± 4.5 nm.

2.3. Film preparation

A stock solution of gelatine from porcine skin 6% (w/v) in distilled water was prepared. For that purpose, the gelatine-water mixture was heated in a water bath at 65 °C for 25 minutes. Then, an amount of glycerol equivalent to 30% (w/w) of the gelatine powder previously dissolved was added, and the resulting solution was cooled at room temperature to 35 °C. With this stock were prepared several film-forming solutions that contained 1%, 2% and 3% (w/w of gelatine) of free thymol or alternatively of encapsulated thymol. These film-forming solutions were poured into Petri dishes of 4 cm diameter in such a way that every film was made up of 216 mg of gelatine, and then dried at room temperature for 2 days. Finally, the films were manually peeled from the dishes. The films obtained were conditioned for 1 day at room temperature (21 °C) in a closed chamber that contained a saturated solution of $Mg(NO_3)_2$.

2.4. Light absorbance, transparency, thickness and thymol content

Light absorbance and transparency were determined according to Dick et al. (2015) using a spectrophotometer (Spekol 1500, Analytik Jena AG, Jena, Germany) at selected wavelengths between 200 to 800 nm. For this purpose, rectangular pieces of film were placed in the spectrophotometer test cell, while an empty cell was used as reference. The transparency of the films was calculated according to the following equation:

$$\text{Transparency} = A_{600}/\text{Th} \quad (1)$$

Where A_{600} is the absorbance of the film sample at 600 nm and *Th* is the film thickness (mm).

The film thickness was measured using a digital micrometre (Model MDC-25PX, Mitutoyo C., Kanagawa, Japan), with a measuring range of 0-25 mm and a precision of ± 1 μm. The film thickness was measured in five different areas, one of them in the centre of the film and the other four around the film perimeter.

To check the amount of thymol that remained in the films after the solvent evaporation of the film-forming solution, a preliminary thymol release assay was performed to determine the time required for all the thymol contained in the films to be released into an ethanol solution (96%). Ethanol was selected for this experiment to ensure the diffusion of thymol, which is highly soluble in this solvent. For that purpose, every type of film produced was placed in an amber vial, filled with ethanol at 40 °C under orbital stirring for 72 hours. To calculate the

amount of thymol in the ethanol, an aliquot of 2 mL for each vial was taken at several times and the absorbance at 275 nm was measured. The thymol concentration in the sample was determined by preparing a calibration curve with known concentrations of thymol in ethanol. The possible interferences produced by the film matrix were corrected using films without thymol as blank. The amount of thymol released at 40 °C after 24 hours was considered to be all the thymol contained in the films. The amount of thymol released into the ethanol was compared with the amount of thymol incorporated into the film-forming solution to calculate the thymol loss during the drying step.

2.5. Mechanical properties of the gelatine films

The measurement of the puncture strength (PS) and puncture deformation (PD) of the gelatine films was carried out using a Texture Analyser TA.XT.plus (Stable Microsystems, Surrey, UK) equipped with a load cell of 5 kg and a probe of 5 mm diameter (P/5S). For this purpose, the films were cut into strips of 40 x 20 mm and attached in the assay platform between two plates. Through the two plates a hole of 1 cm allows contact between the probe and the film sample, so that the probe can stretch the film until it breaks. The probe velocity was 1 mm s^{-1} and the PS and PD parameters were calculated according to the following equations (Pérez-Mateos et al., 2009) :

$$\mathrm{PS} = \mathrm{Fm}/\mathrm{Th} \qquad (2)$$

$$\mathrm{PD} = \left(\sqrt{\mathrm{D}^2 + \mathrm{R}^2} - \mathrm{R}\right)/\mathrm{R} \qquad (3)$$

Where *Fm* is the maximum force applied before the film breaks, *Th* is the film thickness, *D* is the distance covered by the probe while it is in contact with the film until the film is broken and *R* is the radius of the orifice in the plates.

2.6. Thymol release from gelatine films loaded with PLA nanoparticles

The thymol released from the gelatine films into the liquid medium was evaluated in accordance with ASTM D4754-98 (ASTM, 2006). In this case only the films loaded with PLA-thymol nanoparticles were evaluated, and the release of the thymol was carried out at three different temperatures (5 °C, 20 °C and 40 °C), using ethanol (96%) as the food simulant. Ethanol has been commonly used as a fatty food simulant by other authors to study the release of different non-water soluble active agents from films (Manzanarez-López et al., 2011; Ortiz-Vazquez et al., 2011; Rodríguez-Martínez et al., 2016). For this purpose, each film tested

was cut into four round discs (2 cm of diameter). These four discs were immobilized using a stainless-steel wire and separated one from another using glass beads of 5 mm diameter. Then, the film pieces were placed in amber vials that were filled with 20 mL of ethanol. The ethanol volume/film area was 0.8 mL cm^{-2}, which is within the volume-to-surface area range, from 155 to 0.31 mL cm^{-2}, recommended by the ASTM D4754-98. The release of thymol from the films to the liquid medium was measured at several times, using the technique explained in section 2.4. After every measurement, the ethanol sample was returned to the vials.

To calculate de diffusion coefficient of the thymol (*D*), the analytical solution of Crank (1979) (equation 4) to study the diffusion phenomena in a plane sheet was used. To apply this equation, it was assumed there was no reaction between thymol and the film matrix, a homogeneous concentration distribution of thymol, that the amount of solvent can be considered infinite, negligible edge effect, and therefore a unidirectional diffusion of the active agent from the surface of the film into the liquid).

$$\frac{M_t}{M_\infty} = 1 - \sum_{n=0}^{\infty} \frac{8}{(2n+1)^2\pi^2} e^{\{-D(2n+1)^2\pi^2 t/4L^2\}} \qquad (4)$$

Where M_t is the amount of thymol released at each time, M_∞ is the amount of thymol released after infinite time and *L* is the half-thickness of the films tested. If instead of considering all the data collected during this experiment, only the values of $M_t/M_\infty > 0.4$ are taken, equation 4 can be rewritten as the following linear regression model (Han et al., 2000):

$$\ln\left(1 - \frac{M_t}{M_\infty}\right) = ln\frac{8}{\pi^2} - \frac{D\pi^2 t}{4L^2} \qquad (5)$$

When the first term of this equation is plotted vs time, the *D* parameter can be calculated from the slope.

To assess the dependence of the thymol diffusion on temperature, the activation energy (E_a) was calculated. For that purpose, the Arrhenius model was applied using the *D* values obtained from equation (5) (Limm and Hollifield, 1996):

$$lnD = lnD_0 - \frac{E_a}{RT} \qquad (6)$$

Where D_0 is a constant, *T* is the temperature tested (K) and *R* is the universal gas constant.

2.7. Scanning electron microscopy

The micrographs of the transversal section of the films were performed according to Kadam et al. (2015) and using a scanning electron microscope (JSM-6610LV, JEOL, Tokyo, Japan). To

obtain these micrographs, the films were lyophilized and cut into 1x1 cm squares. These samples were mounted perpendicularly on aluminium stubs and covered with gold. The microscope was operated with a voltage of 20 kV.

2.8. Antimicrobial properties of the gelatine films

To test the antimicrobial properties of the gelatine films with thymol and the nanoparticles loaded with thymol, 1 g pieces of apple (Royal Gala apple variety) were inoculated with the non-pathogenic strain of *E. coli* CECT 101 (CECT, *Colección Española de Cultivos Tipo*, Spanish Type Culture Collection). This strain was cultured using NB (Nutrient Broth) medium, supplemented with 2% agar and incubated at 30 °C for 48 hours. It was then incubated in NB liquid for 10 hours at 30 °C under orbital stirring at 26.17 rad s^{-1}.

The apple pieces were inoculated with 0.1 mL of this solution, containing an *E. coli* concentration of 10^5 CFU mL^{-1}. These apple pieces were then covered with the gelatine films and sealed using a heat-sealing machine. Every piece of apple sealed was placed in a petri dish and stored at 5 °C for 14 days. To follow the growth of *E. coli* with each type of gelatine film tested, after 3 or 4 days of storage time a sample was taken, the film removed, the apple mixed with 9 mL of NaCl 0.7% and the mixture triturated using a Stomacher (IUL Instruments, Barcelona, Spain) for 120 seconds. Then, the liquid sample obtained was diluted and seeded in NB medium with 2% agar. After 24 hours of incubation at 30 °C the colonies were counted and expressed as $\log_{10}$ CFU mL^{-1}.

2.9. Statistical analysis

Experiments were performed in triplicate and are shown as the mean value ± standard deviation of three independent experiments (n = 3). Least significant differences (LSD) were calculated by Fisher's test to determine significant differences between the tested samples. These analyses were performed using the statistical software Statgraphics® V.15.2.06.

3. RESULTS

3.1. Light absorbance, transparency, thickness and thymol content

After the solvent evaporation of the film-forming solution for 2 days, the films were peeled easily and entirely, not showing a sticky or brittle appearance. The visual aspect of the films is shown in Figure 1. The gelatine films with free thymol are not shown because their appearance was identical to that of the control films. In this Figure it can be observed how the increment in the amount of PLA nanoparticles produced a decrease in the film transparency. This variation in the transparency parameter was also noticed when the film strips were analysed using the

spectrophotometer (Table 1), a rise from 0.48 in the control films to 1.04 in the films with 3% thymol encapsulated in PLA nanoparticles being detected. It is understood that a rise in this value corresponds to a decrease in the film transparency.

Regarding the absorbance values at different wavelengths, is also desirable that a good film can act as a barrier to ultraviolet light, since this is an important starter for the lipid oxidation process (Coupland and McClements, 1996). Most protein-based films have a high capacity to absorb ultraviolet light, due to the presence of amino acids with aromatic side chains, such as tyrosine, tryptophan and phenylalanine. However, the gelatine protein lacks tryptophan and it has a fairly low amount of tyrosine and phenylalanine (Nhari et al., 2011). This results in a relatively low barrier capacity at these wavelengths for the gelatine films in comparison with other protein-based films. Table 1 shows that the control films present an absorbance at 280 nm of 0.808, whereas the gelatine film with 3% thymol in nanoparticles has an absorbance of 1.521, which is a rise of 0.71. Taking into account that PLA does not show particularly high absorbance at this wavelength, this increase could be produced by the addition of thymol, which exhibits an absorption spectrum with a major peak at 274 nm (Hajimehdipoor et al., 2010). Furthermore, the gelatine films with 3% free thymol showed an absorption profile similar to that found for the control film, which suggests the total evaporation of the thymol during the film-forming solvent evaporation step. The gelatine films with 2% and 1% free thymol showed the same absorbance value as that found for the gelatine film with 3% free thymol.

With respect to the thickness, a slight increase was detected when the nanoparticles were added, in particular, when the thickness value for the control films is compared with the value for the 3% nanoparticles gelatine films (Table 1). The addition of free thymol to the film-forming solution produced films with the same thickness value as that of the control films.

The film transparency, absorbance at 280 nm and thickness values obtained suggest that all the free thymol incorporated into the gelatine films was evaporated during the drying of the film-forming solution. This supposition was confirmed when the amount of thymol in these films was tested (Table 1). Films with 3% free thymol lost all their active agent content during the solvent evaporation step. This could be explained by both the high volatility of thymol and the low capacity of gelatine to retain the thymol molecules. In the case of proteins, molecular binding studies carried out by Pan et al. (2014) showed that thymol is able to bind to tyrosine and tryptophan residues in a protein, but as was mentioned previously, the former amino acid

is found at a very low proportion in gelatine, and the latter is not present at all, due to it is being degraded during the production of the gelatine (Hafidz et al., 2011). In addition, when thymol encapsulated in PLA nanoparticles was incorporated into the film-forming solution, the thymol loss was also noticeable, but a proportion of the added thymol remained in the dried film (Table 1). It is to be expected that during the drying of the film-forming solution a part of the thymol in the nanoparticles is continuously diffusing into the aqueous medium and is then evaporated together with the solvent. This effect is likely to be enhanced at the beginning of the drying step, when the amount of water in the film-forming solution is large enough to produce a major release of thymol from the nanoparticles to the water.

Taking into account the total evaporation of the free thymol in the gelatine films during the film-forming solution drying step, in the following experiments only the gelatine films loaded with PLA-thymol nanoparticles were considered.

3.2. Gelatine films: mechanical properties

The PS and PD values of the gelatine films are shown in Figure 2. The PS parameter indicates the mechanical resistance of a film, and in this case, the addition of nanoparticles loaded with thymol did not produce any statistically significant variation ($p < 0.05$). Furthermore, the PD parameter, which is a measurement of the film's elasticity, was influenced by the addition of PLA nanoparticles, a statistically significant difference appearing between the control film and those with 2% and 3% thymol in PLA nanoparticles. During the film drying, the protein chains come closer and establish non-covalent interactions with one another. In this type of film, the glycerol and water avoid the excessive structuration of the film matrix, allowing some degree of flexibility. In this case, nanoparticles could be occupying places within the film matrix where the glycerol and the water had previously accumulated, replacing them and leading to a decrease in the flexibility of the material. In any case, the decrease in the PD parameter due to the addition of the nanoparticles could be considered slight, from 37.2 ± 7.0% in the control film to 26.5 ± 6.2% in the case of the gelatine film with 3% thymol in nanoparticles.

3.3. Scanning electron microscopy

The micrographs of the film matrix are shown in Figure 3. In these micrographs it can be observed how the films showed a highly homogeneous transverse section, even in the case of the gelatine films with 3% thymol encapsulated in nanoparticles. However, the smoothest cross section area was that found for the gelatine control film, and a slight decrease in this

285 homogeneity can be observed as the amount of encapsulated thymol increased. This slight
286 difference between the micrographs shown in Figure 3D and 3A could explain the loss of
287 elasticity that was appreciated when the mechanical properties of the films were tested.

288 **3.4. Thymol release from gelatine films loaded with PLA-thymol nanoparticles**

289 The thymol release profiles for the gelatine films with different thymol-loaded nanoparticle
290 concentrations were very similar to each other at every temperature tested, regardless of the
291 amount of thymol incorporated into the films (Figure 4). Furthermore, changes in temperature
292 produced variations in the shape of the curves for the three thymol concentrations tested, as
293 was expected. In particular, at 40 °C, all the thymol contained in the nanoparticles was
294 released in two hours independently of the concentration of thymol. At 20 °C, almost all the
295 thymol was released in 23 hours, and at 5 °C all the thymol incorporated was released in 71
296 hours. The differences in the shape of the thymol release profiles at each temperature tested
297 could be mainly due to the effect of the temperature on thymol solubility. So, at 40.4 °C the
298 thymol solubility value is 946 mg mL^{-1}, while at 30.9 °C this value decreases to 744 mg mL^{-1}
299 (Villanueva Bermejo et al., 2015). The diffusion coefficients calculated using equation (5) for
300 these release curves are shown in Table 2. The experimental data obtained fitted to this
301 equation with a high coefficient of determination ($R^2 > 0.99$). As is shown in this Table, the
302 value of these coefficients decreased by a similar degree from 40 °C to 20 °C as from 20 °C to 5
303 °C, which suggests that the temperature does not affect the thymol release mechanism, and
304 that the drop in the thymol release rate is caused mainly by a decrease in thymol solubility.
305 Furthermore, the diffusion coefficient decreased by one order of magnitude when the
306 temperature fell from 40 °C to 5 °C, which was also seen by other authors working with thymol
307 and zein films (Kashiri et al., 2017). In addition, similar diffusion values to those shown in Table
308 2 were reported by Ramos et al. (2014), studying thymol release from polypropylene films
309 using ethanol 95% as food simulant and at 40 °C. In this case, these authors reported a
310 diffusion coefficient of 1.01 x 10^{-10} cm^2 s^{-1}.

311 To study the temperature dependence of the diffusion values obtained, an Arrhenius plot was
312 carried out (Figure 5). The diffusion values shown in Table 2 were fitted to the Arrhenius
313 equation with a high coefficient of determination ($R^2 > 0.99$), which suggest that the diffusion
314 of encapsulated thymol into the gelatine films can be explained by the Arrhenius activation
315 model. Therefore, the diffusion process is driven mainly by the amount of energy provided to
316 the medium, with no structural modification in the film matrix due to the temperature
317 involved. The activation energies calculated from Figure 5 are shown in Table 2, and as was

318 expected, variations in the concentration of encapsulated thymol added to the films did not
319 produce a great variation in the value of this parameter.

320

321 **3.5. Antimicrobial capacity of the gelatine films loaded with thymol**

322 The effect of the gelatine films with PLA nanoparticles loaded with thymol is shown in Figure 6.

323 Films loaded with encapsulated thymol at 3% and 2% exhibited a similar, low antimicrobial
324 capacity during the first 3 days of storage, but at the sixth day the difference between these
325 two samples was noticeable: the gelatine films loaded with 3% encapsulated thymol decreased
326 the CFU g^{-1} value to 1.95, while in the case of the films loaded with 2% encapsulated thymol,
327 the CFU g^{-1} value decreased to 3.9. During the following days, the decrease in the CFU value
328 was more pronounced in the 2% films, whilst it remained relatively constant for the 3% film. At
329 the end of the storage time, a CFU g^{-1} value of 2.0 was found for the 2% films, while a decrease
330 to 1.5 CFU g^{-1} was measured for the 3% films. It should be expected that the release of thymol
331 from the film to the surface of a food with a relatively high-water content, such as a piece of
332 apple, will be slower than the relatively fast release of thymol to ethanol shown in section 3.4.
333 The reason for this difference in diffusivity is mainly due to the low solubility of thymol in
334 water. This long-term effect is desirable and could explain the reduction in CFUs after 6 days of
335 storage for the pieces of apple covered with 3% and 2% PLA-thymol nanoparticles gelatine
336 films. The antimicrobial effect of the PLA-thymol nanoparticles on *E. coli*-inoculated pieces of
337 apple was tested in a recent study (Marcet et al., 2018), and these antimicrobial properties
338 were found to be slightly worse than those shown by the gelatine films loaded with the same
339 nanoparticles. In the case of the PLA-thymol nanoparticles without film, the amount of thymol
340 encapsulated was 0.5 mg mL^{-1} in the case of the best result obtained, while the concentration
341 of thymol in the PLA-thymol nanoparticles included in the gelatine films was higher than that
342 measured in the PLA-thymol nanoparticles without film, even taking into consideration the
343 evaporation of thymol during the film-forming solution drying step. This could explain the
344 better antimicrobial capacity observed when the PLA-thymol nanoparticles were incorporated
345 into films.

346

347 **4. CONCLUSIONS**

348 The amount of thymol evaporated during the production of protein-based films is a subject
349 that has barely been addressed in this type of packaging materials, and it could have a major

impact on the costs associated with their production, especially considering that this problem is likely to be common to the use of other volatile essential oils. In this study, the total evaporation of non-encapsulated thymol from the gelatine films during the drying step could be due to both to the relatively low amount of thymol added to the film-forming solution and also to the particular amino acid composition of the gelatine proteins; the former is recommendable, since it reduces the weakening effect exerted by the thymol on the mechanical properties of the films, and the latter is very difficult to avoid. In any case, the incorporation of thymol in the form of PLA-thymol nanoparticles in the film-forming solution resulted in the production of solid gelatine films with the active agent present in the film matrix. This thymol that remains in the film matrix showed antimicrobial properties, and its impact on the mechanical properties of the materials produced can be considered slight.

5. REFERENCES

Arfat, Y.A., Benjakul, S., Prodpran, T., Sumpavapol, P., Songtipya, P., (2014). Properties and antimicrobial activity of fish protein isolate/fish skin gelatin film containing basil leaf essential oil and zinc oxide nanoparticles. Food Hydrocolloids 41, 265-273.

ASTM D 4754-98, (2006). Standard Test Method for Two-Sided Liquid Extraction of Plastic Materials Using FDA Migration Cell. Annual Book of ASTM Standards: Conshohocken, PA. vols. 08–02.

Bonilla, J., Atarés, L., Vargas, M., Chiralt, A., (2013). Properties of wheat starch film-forming dispersions and films as affected by chitosan addition. Journal of Food Engineering 114(3), 303-312.

Coupland, J.N., McClements, D.J., (1996). Lipid oxidation in food emulsions. Trends in Food Science & Technology 7(3), 83-91.

Crank, J., (1979). *The mathematics of diffusion*. Oxford university press.

Dalmolin, L.F., Khalil, N.M., Mainardes, R.M., (2016). Delivery of vanillin by poly(lactic-acid) nanoparticles: Development, characterization and in vitro evaluation of antioxidant activity. Materials Science and Engineering: C 62, 1-8.

Dang, K.M., Yoksan, R., (2016). Morphological characteristics and barrier properties of thermoplastic starch/chitosan blown film. Carbohydrate Polymers 150, 40-47.

Del Nobile, M., Conte, A., Incoronato, A., Panza, O., (2008). Antimicrobial efficacy and release kinetics of thymol from zein films. Journal of Food Engineering 89(1), 57-63.

Dhall, R., (2013). Advances in edible coatings for fresh fruits and vegetables: a review. Critical Reviews in Food Science and Nutrition 53(5), 435-450.

Dick, M., Costa, T.M.H., Gomaa, A., Subirade, M., de Oliveira Rios, A., Flôres, S.H., (2015). Edible film production from chia seed mucilage: effect of glycerol concentration on its physicochemical and mechanical properties. Carbohydrate Polymers 130, 198-205.

Etxabide, A., Uranga, J., Guerrero, P., de la Caba, K., (2017). Development of active gelatin films by means of valorisation of food processing waste: A review. Food Hydrocolloids 68, 192-198.

Hafidz, R., Yaakob, C., Amin, I., Noorfaizan, A., (2011). Chemical and functional properties of bovine and porcine skin gelatin. International Food Research Journal 18, 813-817.

391 Hajimehdipoor, H., Shekarchi, M., Khanavi, M., Adib, N., Amri, M., (2010). A validated high
392 performance liquid chromatography method for the analysis of thymol and carvacrol in
393 Thymus vulgaris L. volatile oil. Pharmacognosy Magazine 6(23), 154-158.
394 Han, J.H., Krochta, J.M., Hsieh, Y.-L., Kurth, M.J., (2000). Mechanism and characteristics of
395 protein release from lactitol-based cross-linked hydrogel. Journal of Agricultural and Food
396 Chemistry 48(11), 5658-5665.
397 Kadam, S.U., Pankaj, S.K., Tiwari, B.K., Cullen, P.J., O'Donnell, C.P., (2015). Development of
398 biopolymer-based gelatin and casein films incorporating brown seaweed Ascophyllum
399 nodosum extract. Food Packaging and Shelf Life 6, 68-74.
400 Kashiri, M., Cerisuelo, J.P., Domínguez, I., López-Carballo, G., Muriel-Gallet, V., Gavara, R.,
401 Hernández-Muñoz, P., (2017). Zein films and coatings as carriers and release systems of Zataria
402 multiflora Boiss. essential oil for antimicrobial food packaging. Food Hydrocolloids 70, 260-268.
403 Kavoosi, G., Dadfar, S.M.M., Purfard, A.M., (2013). Mechanical, physical, antioxidant, and
404 antimicrobial properties of gelatin films incorporated with thymol for potential use as nano
405 wound dressing. Journal of Food Science 78(2), E244-E250.
406 Li, K.-K., Yin, S.-W., Yang, X.-Q., Tang, C.-H., Wei, Z.-H., (2012). Fabrication and characterization
407 of novel antimicrobial films derived from thymol-loaded zein–sodium caseinate (SC)
408 nanoparticles. Journal of Agricultural and Food Chemistry 60(46), 11592-11600.
409 Limm, W., Hollifield, H.C., (1996). Modelling of additive diffusion in polyolefins. Food Additives
410 & Contaminants 13(8), 949-967.
411 Manzanarez-López, F., Soto-Valdez, H., Auras, R., Peralta, E., (2011). Release of α-Tocopherol
412 from Poly(lactic acid) films, and its effect on the oxidative stability of soybean oil. Journal of
413 Food Engineering 104(4), 508-517.
414 Marcet, I., Weng, S., Sáez-Orviz, S., Rendueles, M., Díaz, M., (2018). Production and
415 characterisation of biodegradable PLA nanoparticles loaded with thymol to improve its
416 antimicrobial effect. Journal of Food Engineering 239, 26-32.
417 Mastromatteo, M., Barbuzzi, G., Conte, A., Del Nobile, M., (2009). Controlled release of thymol
418 from zein based film. Innovative Food Science & Emerging Technologies 10(2), 222-227.
419 Nhari, R., Hafidz, R.M., Che Man, Y., Ismail, A., Anuar, N., (2011). Chemical and functional
420 properties of bovine and porcine skin gelatin. International Food Research Journal 18(2), 813-
421 817.
422 Nouri, L., Nafchi, A.M., (2014). Antibacterial, mechanical, and barrier properties of sago starch
423 film incorporated with betel leaves extract. International journal of biological macromolecules
424 66, 254-259.
425 Ortiz-Vazquez, H., Shin, J., Soto-Valdez, H., Auras, R., (2011). Release of butylated
426 hydroxytoluene (BHT) from Poly(lactic acid) films. Polymer Testing 30(5), 463-471.
427 Pan, K., Chen, H., Davidson, P.M., Zhong, Q., (2014). Thymol nanoencapsulated by sodium
428 caseinate: physical and antilisterial properties. Journal of Agricultural and Food Chemistry
429 62(7), 1649-1657.
430 Park, H.Y., Kim, S.J., Kim, K.M., You, Y.S., Kim, S.Y., Han, J., (2012). Development of Antioxidant
431 Packaging Material by Applying Corn-Zein to LLDPE Film in Combination with Phenolic
432 Compounds. Journal of Food Science 77(10), E273-E279.
433 Pérez-Mateos, M., Montero, P., Gómez-Guillén, M., (2009). Formulation and stability of
434 biodegradable films made from cod gelatin and sunflower oil blends. Food Hydrocolloids 23(1),
435 53-61.
436 Ramos, M., Beltrán, A., Peltzer, M., Valente, A.J.M., Garrigós, M.d.C., (2014). Release and
437 antioxidant activity of carvacrol and thymol from polypropylene active packaging films. LWT -
438 Food Science and Technology 58(2), 470-477.
439 Rodríguez-Martínez, A.V., Sendón, R., Abad, M.J., González-Rodríguez, M.V., Barros-Velázquez,
440 J., Aubourg, S.P., Paseiro-Losada, P., Rodríguez-Bernaldo de Quirós, A., (2016). Migration
441 kinetics of sorbic acid from polylactic acid and seaweed based films into food simulants. LWT -
442 Food Science and Technology 65, 630-636.

443 Roussaki, M., Gaitanarou, A., Diamanti, P.C., Vouyiouka, S., Papaspyrides, C., Kefalas, P., Detsi,
444 A., (2014). Encapsulation of the natural antioxidant aureusidin in biodegradable PLA
445 nanoparticles. Polymer Degradation and Stability 108, 182-187.
446 Tongnuanchan, P., Benjakul, S., Prodpran, T., (2014). Structural, morphological and thermal
447 behaviour characterisations of fish gelatin film incorporated with basil and citronella essential
448 oils as affected by surfactants. Food Hydrocolloids 41, 33-43.
449 Villanueva Bermejo, D., Angelov, I., Vicente, G., Stateva, R.P., Rodriguez García-Risco, M.,
450 Reglero, G., Ibañez, E., Fornari, T., (2015). Extraction of thymol from different varieties of
451 thyme plants using green solvents. Journal of the Science of Food and Agriculture 95(14),
452 2901-2907.

453

***Conflict if Interest form**

Conflict of Interest and Authorship Conformation Form

Please check the following as appropriate:

- All authors have participated in conception and design, or analysis and interpretation of the data; drafting the article or revising it critically for important intellectual content; and approval of the final version.

- This manuscript has not been submitted to, nor is under review at, another journal or other publishing venue.

- The authors have no affiliation with any organization with a direct or indirect financial interest in the subject matter discussed in the manuscript

Figure 1

Figure 1.

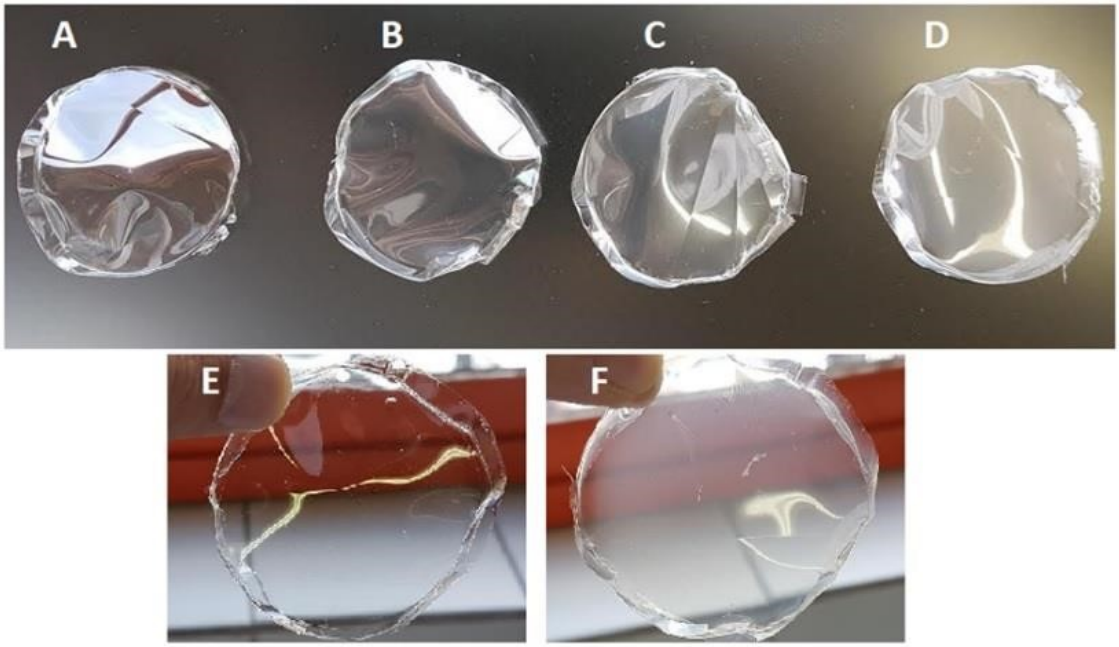

Figure 2

Figure 2.

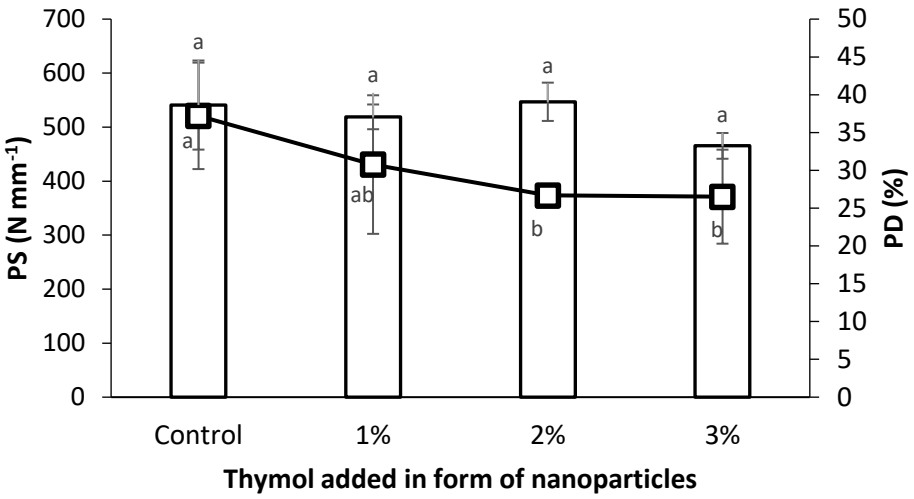

Figure 3

Figure 3.

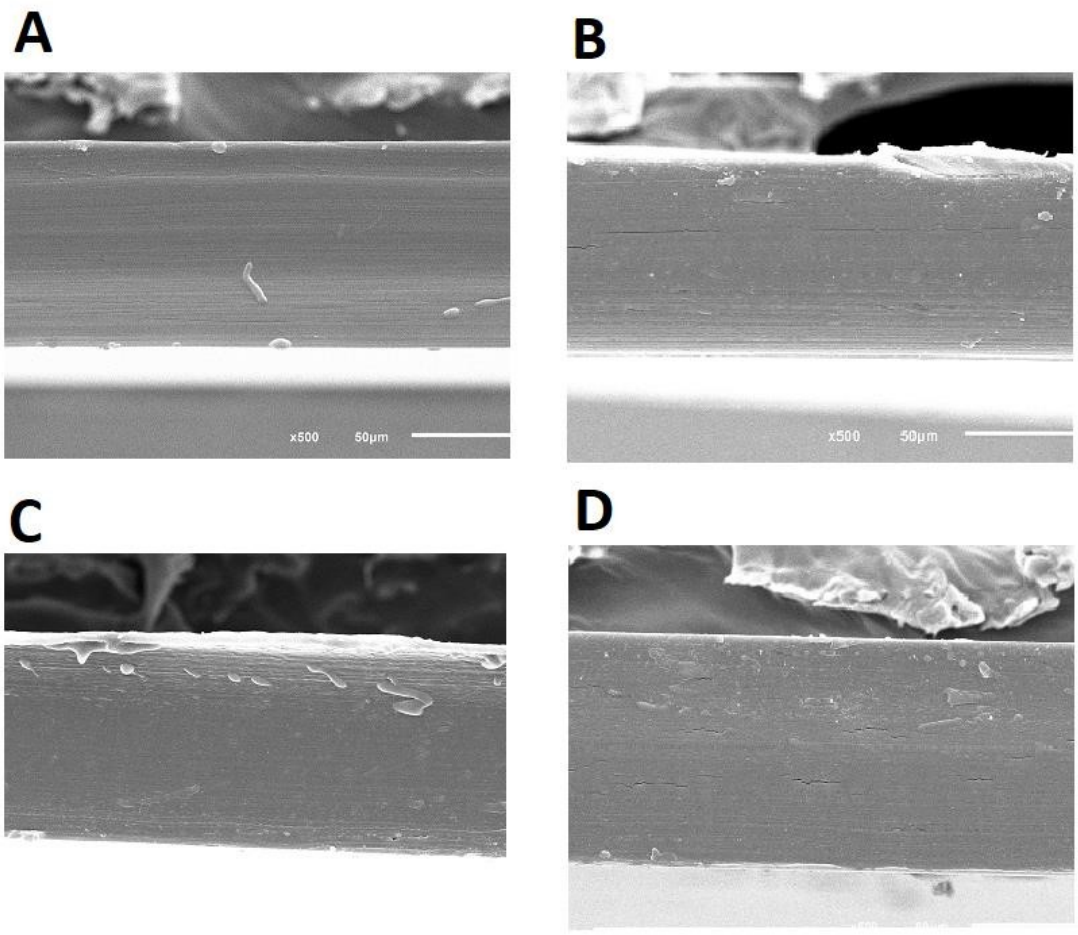

Figure 4

Figure 4.

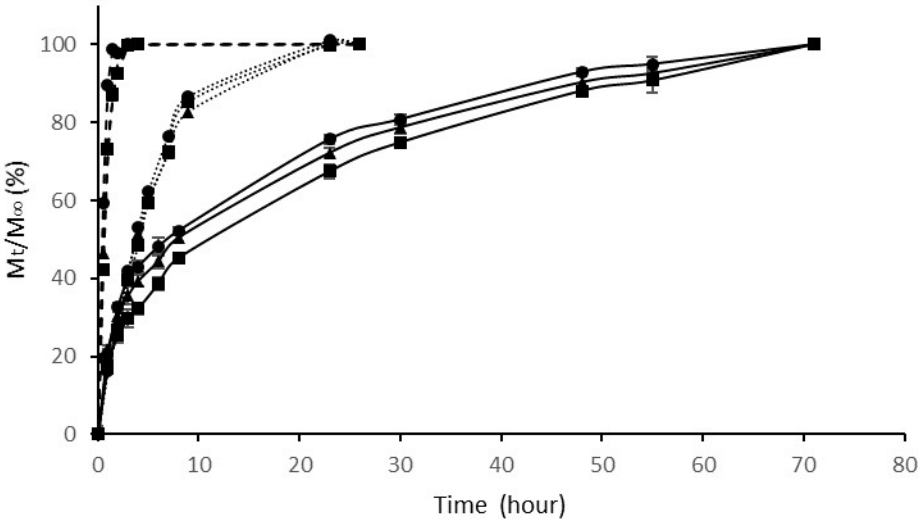

Figure 5

Figure 5.

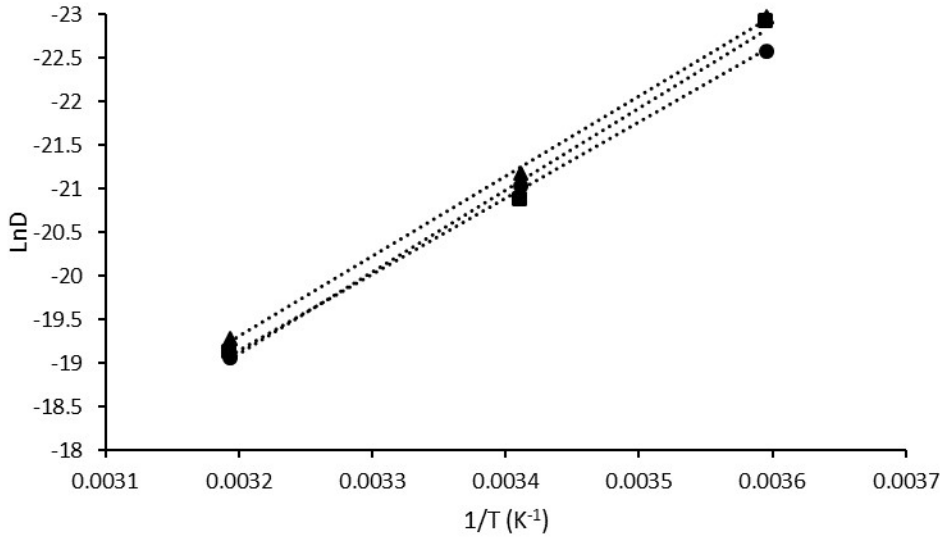

Figure 6

Figure 6.

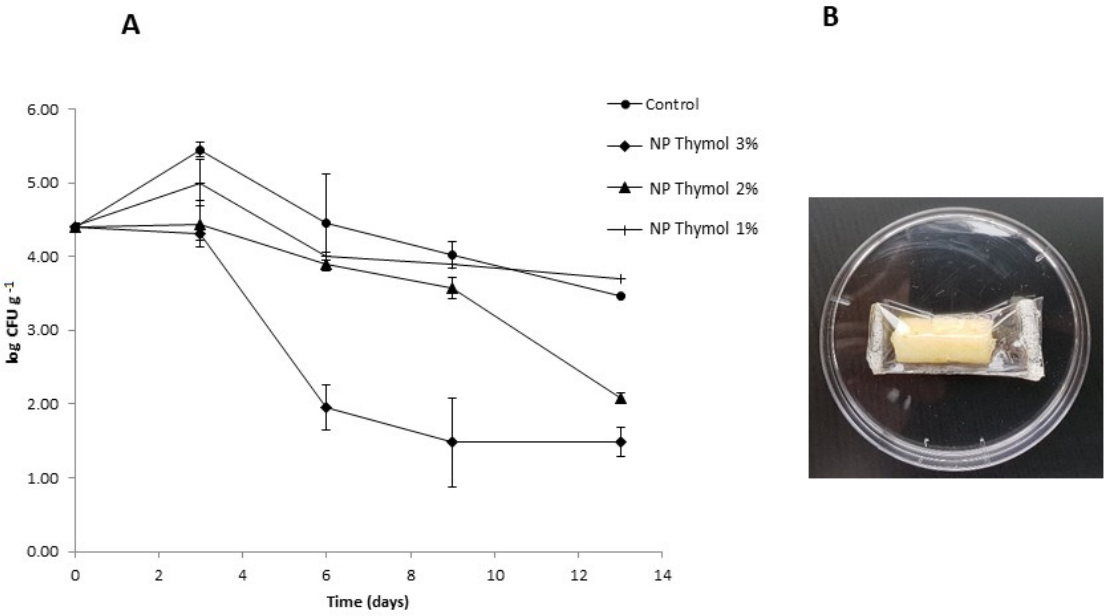

Figure Captions

Figure 1. Visual appearance of the films obtained. A and E. Gelatine films control, without the addition of thymol. B. Gelatine film with 1% of thymol encapsulated in nanoparticles. C. Gelatine film with 2% of thymol encapsulated in nanoparticles. D and F. Gelatine film with 3% thymol encapsulated in nanoparticles

Figure 2. Mechanical properties of the tested films. PS parameter is represented with bars, while PD is represented with squares. For each parameter, different letters indicate statistically significant difference ($p < 0.05$).

Figure 3. Micrographs of the transverse section of the gelatine films loaded with PLA-thymol nanoparticles at 500x. A. Control film. B. Gelatine film with 1% thymol. C. Gelatine film with 2% thymol. D. Gelatine film with 3% thymol

Figure 4. Diffusion kinetics of thymol in gelatine films loaded with PLA-thymol nanoparticles. Broken line, 40 °C. Dotted line, 20 °C. Continuous line, 5 °C. Circles, gelatine film with 1% thymol. Triangle shape, gelatine film with 2% thymol. Squares, gelatine film with 3% thymol.

Figure 5. Arrhenius plot for the release of thymol from the gelatine films with thymol encapsulated in nanoparticles. Circles, gelatine film with 1% thymol. Triangle shape, gelatine film with 2% thymol. Squares, gelatine film with 3% thymol.

Figure 6. A. Growth of *E. coli* CECT 101 on apples covered with gelatine films that have PLA-thymol nanoparticles incorporated. B. Sample of apple piece covered with a gelatine film that has a 3% PLA-thymol nanoparticle content.

Table 1

Table 1. Film thickness, transparency, absorbance at different wavelengths and amounts of thymol remaining after the drying of the film-forming solution.

	Thickness (mm)	Absorbance									Transparency	Thymol that remains in the film (%)
		200 nm	250 nm	280 nm	300 nm	400 nm	500 nm	600 nm	700 nm	800 nm		
Control	0.094 ± 0.007[a]	2.407	0.894	0.808	0.181	0.056	0.046	0.045	0.044	0.043	0.48	--
NP 1%	0.102 ± 0.002[ab]	> 3.0	1.147	1.059	0.289	0.112	0.085	0.072	0.065	0.064	0.71	11.6 ± 0.7[a]
NP 2%	0.102 ± 0.003[ab]	> 3.0	1.198	1.189	0.323	0.132	0.099	0.083	0.075	0.069	0.81	14.3 ± 1.0[b]
NP 3%	0.110 ± 0.003[b]	2.846	1.496	1.521	0.452	0.196	0.142	0.115	0.102	0.09	1.04	18.5 ± 1.2[c]
Thymol free 3%	0.096 ± 0.005[a]	2.455	0.880	0.838	0.191	0.058	0.045	0.045	0.044	0.043	0.46	0

Different letters in the same column indicate significant differences ($P<0.05$).

Table 2

Table 2. Diffusion coefficients of thymol released from gelatine films loaded with PLA-thymol nanoparticles into ethanol at 5, 20 and 40 °C, and activation energies for the diffusion of thymol from the gelatine films.

Films with nanoparticles loaded with thymol	**Diffusion coefficients ($cm^2 s^{-1}$)**			**Activation Energies ($KJ\ mol^{-1}$)**
	5 °C	20 °C	40 °C	
3%	1.10 (x 10^{-10})	8.60 (x 10^{-10})	4.90 (x 10^{-9})	78.13
2%	1.05 (x 10^{-10})	6.33 (x 10^{-10})	4.22 (x 10^{-9})	76.20
1%	1.58 (x 10^{-10})	7.38 (x 10^{-10})	5.27 (x 10^{-9})	72.62